Global Change Biology

WILEY

Global Change Biology

RESEARCH ARTICLE

Water Limits Radial Tree Growth More Than Light in an Everwet Subtropical Forest

Laura E. Boeschoten[1,2,3] | Chris M. Smith-Martin[4] | Jose A. Medina-Vega[5] | Kristina J. Anderson-Teixeira[5,6] | Luis A. Esbrí Ruiz[1] | Rebecca A. Montgomery[7] | Monique Picón[8] | Mukund P. Rao[9,10] | Tana E. Wood[11] | Xiangtao Xu[12] | Jess K. Zimmerman[8] | María Uriarte[1]

[1]Department of Ecology, Evolution and Environmental Biology, Columbia University, New York, New York, USA | [2]Q-ForestLab, Department of Environment, Faculty of Bioscience Engineering, Ghent University, Ghent, Belgium | [3]Belgian Climate Centre, Uccle, Belgium | [4]Department of Plant and Microbial Biology, University of Minnesota, St. Paul, Minnesota, USA | [5]Forest Global Earth Observatory, Smithsonian Tropical Research Institute, Washington, District of Columbia, USA | [6]Conservation Ecology Center, Smithsonian National Zoo & Conservation Biology Institute, Front Royal, Virginia, USA | [7]Department of Forest Resources, University of Minnesota, St. Paul, Minnesota, USA | [8]Department Environmental Sciences, University of Puerto Rico, San Juan, Puerto Rico | [9]Tree-Ring Laboratory, Lamont-Doherty Earth Observatory of Columbia University, Palisades, New York, USA | [10]CREAF, Bellatera (Barcelona), Spain | [11]USDA Forest Service, International Institute of Tropical Forestry, Río Piedras, Puerto Rico | [12]Department of Ecology and Evolutionary Biology, Cornell University, Ithaca, New York, USA

Correspondence: Laura E. Boeschoten (laura.boeschoten@ugent.be)

Received: 23 March 2026 | **Revised:** 14 June 2026 | **Accepted:** 29 June 2026

Keywords: carbon allocation | point dendrometer | seasonality | sink-limitation | subtropical forest | tree growth

ABSTRACT

Everwet tropical forests, defined by the absence of a pronounced dry season, are globally significant carbon sinks, covering roughly 80% of Southeast Asian tropical forests, 30% of the Amazon basin, and 10% of the Congo Basin. Yet the climatic drivers of stem radial growth in these ecosystems remain understudied. The prevailing hypothesis is that growth is primarily light-limited, as persistent cloud cover constrains photosynthesis. Evaluating this assumption is critical as climate projections for the humid tropics point towards rising atmospheric evaporative demand, episodic drought, and reduced cloud cover, conditions whose net effect on woody growth remains unresolved. To address this gap, we deployed automated point dendrometers on 35 trees in an everwet subtropical forest with 3500 mm mean annual precipitation and no pronounced rainfall seasonality, collecting 2 years of hourly radial stem growth data alongside concurrent measurements of soil moisture, vapor pressure deficit (VPD), and light availability. Contrary to the prevailing light-limitation hypothesis, soil moisture and atmospheric evaporative demand were the primary determinants of both whether and how much growth occurred on any given day, even under these perennially wet conditions. Light availability and photoperiod enhanced growth magnitude when water was not limiting, but their effects were consistently smaller. Droughts occurring during the wetter, high-growth months had the greatest negative impact on annual stem increment, potentially reducing annual growth to just 20% of current levels. These results challenge long-standing assumptions of light-limited stem growth in everwet forests, which is critical for improving model projections of forest responses to climate change. Broader validation across tropical forests, combined with direct physiological measurements of carbon uptake and storage, will be essential to evaluate our working hypothesis that radial growth in these everwet ecosystems is ultimately more constrained by water availability than by carbon supply.

1 | Introduction

Tropical forests play a crucial role in carbon uptake and stabilization of the global climate (Pan et al. 2024; Anderson-Teixeira et al. 2021). However, the persistence of this carbon sink is increasingly uncertain as a warming climate increasingly changes growth conditions (Hubau et al. 2020). Rising atmospheric CO_2 concentrations (Zwartsenberg et al. 2025), higher temperatures (Trew et al. 2024; Feron et al. 2024), more frequent and prolonged droughts (Feron et al. 2024) and increasing aridity (Fang et al. 2022) are reshaping growth conditions across the tropics. Meanwhile, we still have a limited mechanistic understanding of how temporal climate variability influences radial stem growth and consequently, woody biomass accumulation (Peters, Kaewmano, et al. 2023; Zhou et al. 2023). This knowledge gap is particularly pronounced in everwet forests, for example, those that experience no month with less than 100 mm of rain. The absence of strong rainfall seasonality limits the formation of distinct tree rings, complicating the development of growth chronologies to study climate-growth relationships (Zuidema et al. 2022). Long-term tree censuses offer an alternative, but data from everwet ecosystems is also scarce with only a few studies measuring growth sub-annually to study climate-growth relations (Clark et al. 2010). Consequently, everwet forests remain underrepresented in the literature, limiting our insights into the drivers of growth in these highly productive systems (Muller-Landau et al. 2021). This knowledge gap is especially important to address given that everwet forests constitute roughly 80% of Southeast Asian tropical forests (Luo et al. 2024; Huke 1982), 30% of the Amazon basin (Luo et al. 2024; Anderson et al. 2018) and 10% of the Congo Basin (Luo et al. 2024).

This limited understanding of climate-growth relationships is reflected in a major uncertainty in the land surface components of Earth System Models, our primary means of projecting the long-term effects of global climate warming (Canadell et al. 2021). In process-based dynamic vegetation models, growth is directly governed by photosynthesis, quantified as gross primary productivity (GPP) (Fatichi et al. 2019; Friend et al. 2019; Koven et al. 2020; Xu et al. 2016; Fatichi et al. 2014). GPP sets the total available carbon pool and after accounting for respiration, tissue turnover, and carbon storage replenishment, the residual carbon is allocated to tissue growth (Koven et al. 2020). This framework assumes that all post-assimilation processes, including leaf, stem and root biomass production, are solely constrained by photosynthesis, that is, source-limited (Friend et al. 2019; Keenan et al. 2016). Under this paradigm, enhancements to GPP are expected in wet tropical forests via increased atmospheric CO_2 concentrations, reduced cloud cover (and thus increased light availability), and changes in leaf dynamics, leading to increased radial stem growth (Hubau et al. 2020; Zwartsenberg et al. 2025; Green et al. 2020; Knauer et al. 2023; Graham et al. 2003). However, recent empirical studies suggest that radial stem growth is decoupled from GPP, exhibiting a direct sensitivity to temperature and moisture unrelated to photosynthesis (Peters, Kaewmano, et al. 2023; Friend et al. 2019; Wagner et al. 2016; Cabon et al. 2022; Körner 2015). These findings point to the role of sink-limitation, that is, direct constraints on the ability of trees to convert assimilated carbon into biomass. Although the distinction between source- and sink-driven growth may not be absolute (Gessler and Zweifel 2024; Trugman and Anderegg 2025), uncertainty in carbon allocation mechanisms under variable climate conditions is leading to diverging long-term projections of carbon dynamics (Friend et al. 2019; Bonan and Doney 2018; Xu et al. 2024). Current models underestimate water sensitivity and overestimate light sensitivity (Restrepo-Coupe et al. 2017; Eckes-Shephard et al. 2021), and overall overestimate woody productivity (Muller-Landau et al. 2021; Eckes-Shephard et al. 2025). Resolving these discrepancies requires a more mechanistic understanding of the direct sensitivity of stem growth to environmental variability across a broad range of climate conditions (Friend et al. 2019; Eckes-Shephard et al. 2021; Babst et al. 2021).

To test climate-growth relationships at high temporal resolution, automated dendrometers are becoming increasingly popular as they can provide sub-daily measurements of stem growth (Zweifel et al. 2016; Zweifel et al. 2021). Although not yet as widely used in tropical forests, existing studies have underscored the critical role of water, both in the soil and atmosphere (via vapor pressure deficit, VPD), in regulating cell division, expansion and tree growth (Peters, Kaewmano, et al. 2023; Zhou et al. 2023; Spannl et al. 2016; Luse Belanganayi et al. 2024; Niessner et al. 2020; Angoboy Ilondea et al. 2021; Gheyret et al. 2021; Kaewmano et al. 2022). However, like tree ring studies, to our knowledge all high-resolution dendrometer studies to date have been conducted in seasonally dry forests, characterized by dry seasons lasting between three and seven months, with all but one site receiving less than 2000 mm of annual rainfall (Figure S1). In these seasonally dry forests, water scarcity is a well-established constraint on growth, but in everwet forests the environmental controls on growth may be substantially different (Rifai et al. 2018). In forests with over 2000 mm of annual rainfall, even if still seasonal, light is often hypothesized to be more limiting than water for photosynthesis and growth, due to persistent cloud cover (Wagner et al. 2016; Wagner et al. 2014; Yang et al. 2023; Restrepo-Coupe et al. 2013). However, although artificial increases in light availability led to increased branch growth (Graham et al. 2003), this study did not consider the potential negative effect of radiation via co-occurring elevated VPD (Grossiord et al. 2020; Shekhar et al. 2023). In contrast, results from annual stem censuses in a wet forest in Costa Rica (4000 mm rain/year) indicated that wood production can be severely reduced by even slight increases in dryness or temperature (Clark et al. 2010). High resolution dendrometer data now offers the means to resolve these dynamics by capturing stem expansion patterns on an hourly scale (Zhou et al. 2023; Giraldo et al. 2023).

Here, we tested the hypothesis that photosynthetically active radiation is the primary positive driver of stem growth in an everwet subtropical rain forest, measured as photosynthetic photon flux density (PPFD) (Graham et al. 2003; Wagner et al. 2014; van Schaik et al. 1993). To measure radial stem growth, we installed point dendrometers on 35 dominant trees from four species in an everwet subtropical forest in Puerto Rico with an average total rainfall of 3500 mm/year. Although the forest is everwet, rainfall shows some seasonality, ranging from a daily mean of 5.8 mm/day in March to 11.5 mm/day in November (see Section 2). Based on historical irradiance data, we expected higher growth rates from April to August (Hogan et al. 2019), when each month receives about 10% of the total yearly PPFD,

compared to November to February, when monthly PPFD drops to 6%–7%.

We measured hourly stem diameter changes from August 2022 until August 2024, alongside concurrent measurements of radiation (PPFD, mmol/m^2/h), soil moisture (volumetric water content, %), VPD (kPa), and daily photoperiod (number of hours with light). The selected species spanned different life history strategies (early, mid, and late successional), allowing us to assess whether differing photosynthetic and hydraulic traits shaped species-specific responses to climate (Wen et al. 2008; Smith-Martin et al. 2023). Growth was quantified using a zero-growth model that identifies increases in stem diameter as growth only when the tree reaches a new maximum (Zweifel et al. 2016) (illustrated in Figure 2a and Figure S2), assuming limited growth happens during periods of stem shrinkage (Zweifel et al. 2016). In these analyses, we assumed that ample water availability would enable trees to maintain open stomata throughout the day, thereby supporting sustained photosynthesis (Peters, Kaewmano, et al. 2023; Catovsky et al. 2002), and that higher PPFD would consequently result in higher carbon uptake and growth (Graham et al. 2003). Although we did not directly measure photosynthesis, we monitored daily sapflow in all trees during three measurement campaigns, assuming positive sapflow represents open stomates and thus the potential for photosynthesis (Lapa et al. 2017). Lastly, we also modeled growth under several potential climate scenarios to test how a change in climate may affect growth for these species.

2 | Materials and Methods

2.1 | Site and Tree Species

This study was conducted at the Luquillo Experimental Forest in northeastern Puerto Rico, an evergreen forest classified as subtropical wet forest (Ewel and Whitmore 1973). The site has a mean annual temperature of 25.2°C and receives 3500 mm of rainfall annually. Although rainfall is relatively stable, with no month typically receiving <100 mm, half of the annual precipitation occurs between August and December, with generally somewhat lower rainfall between January and March (Figure 1). Rainless periods of 1 week are common (once per year, on average) while longer droughts (>2 weeks) have historically occurred every few years (Scatena 2001). There is also some seasonality in temperature, VPD and light conditions (Figure 1) (Hogan et al. 2019). From June to October, temperatures are 2°C–4°C warmer, leading to elevated VPD. During this period sunlight is also more direct, leading to higher maximum PPFD. Additionally, photoperiod ranges from 11 to 13.5 h of daylight between the cooler months of December and January and the warmer months of June and July, respectively.

In August 2022, we established six plots of 20×20 m adjacent to the existing Luquillo Forest Dynamics Plot (LFDP; 18°200 N, 65°490 N) (Thompson et al. 2002). Two soil probes were installed per plot at a depth of 15 cm to measure soil volumetric water content (%) hourly. Soils in this part of the forest are Zarzal clays with a pH between 4.5 and 6 (O'Connell et al. 2018). Roots are mainly located in the top 20 cm of the soil (Yaffar and Norby 2020), therefore we assume this is the most important depth for water uptake. A nearby climate station at the El Verde Field station, located between 60 and 450 m from the plots, provided hourly climate data on rainfall, relative humidity, temperature, and radiation. VPD was calculated from relative humidity and temperature measurements using the *plantecophys* package (Duursma 2015), assuming an atmospheric pressure of 97.8672 Pa to reflect the elevation (300 m). The LFDP has experienced multiple natural and anthropogenic disturbances over the past century.

Before 1934, portions of the plot were lightly logged and farmed for household agriculture (Thompson et al. 2002), but forest structure and canopy cover have since recovered. In the past few decades, the LFDP has also experienced three major hurricanes: Hugo in 1989, Georges in 1998, and María in September 2017.

Within the six plots, we initially installed point dendrometers on 33 trees of four species: the early successional pioneer *Cecropia schreberiana* (seven individuals), the mid-successional *Guarea guidonia* (five individuals), and the late successional *Dacryodes excelsa* (11 individuals) and *Sloanea berteroana* (10 individuals). These species are among the most dominant of each successional stage in this forest: in the 2016 census of the LFDP, individuals of *C. schreberiana* represented 5.1% of the total basal area, *G. guidonia* 2.8%, *D. excelsa* 10.4% and *S. berteroana* 4.3%. These species have not been investigated for the presence of annual rings, but wood cores did not show clear ring formation upon investigation in the field. Dendrometers were installed over the bark at breast height (1.3 m) and stem radius was monitored hourly for 2 years, from August 2022 until August 2024. Because dendrometers require a settling period, we discarded the first month and analyzed the remaining 709 days. Additionally, point dendrometers were installed on two more individuals of *G. guidonia* in December 2023, providing 244 days of data.

To quantify water status in the same individuals for which we measured growth, we conducted three sapflow and pre-dawn water potential measurement campaigns in July 2023 (high irradiance), November 2023 (peak rainfall), and March 2024 (lowest rainfall). Predawn leaf water potential (Ψ_{pd}), a proxy for plant hydration, was measured on leaves of 23 individuals of *D. excelsa*, *G. guidonia*, and *S. berteroana* using a pressure chamber (PMS Instrument Company). We excluded Ψ_{pd} on *C. schreberiana* due to its insufficient foliage and two *D. excelsa*, one *G. guidonia* and two *S. berteroana* could not be measured due to lack of leaf access. For each measurement, leaves were cut before dawn, immediately sealed in plastic bags to prevent water loss, and transported to the laboratory. There, leaves were placed in the pressure chamber, and pressure was gradually increased until xylem sap appeared at the cut surface. This value was recorded as the leaf water potential.

Additionally, we measured total daily sapflow on 33 individuals using the SFMx Sap Flow Meter (ICT International), which employs the Heat Ratio Method to quantify sapflow through the xylem (one *D. excelsa* and one *G. guidonia* were not included). For each tree, three stainless steel needles (two with thermistors and one as a line heater) were inserted into the sapwood at ~1.3 m height and covered with reflective closed-cell insulation to reduce the influence of external temperature fluctuations. Sapflow was recorded hourly for 4–6 weeks, after which sensors

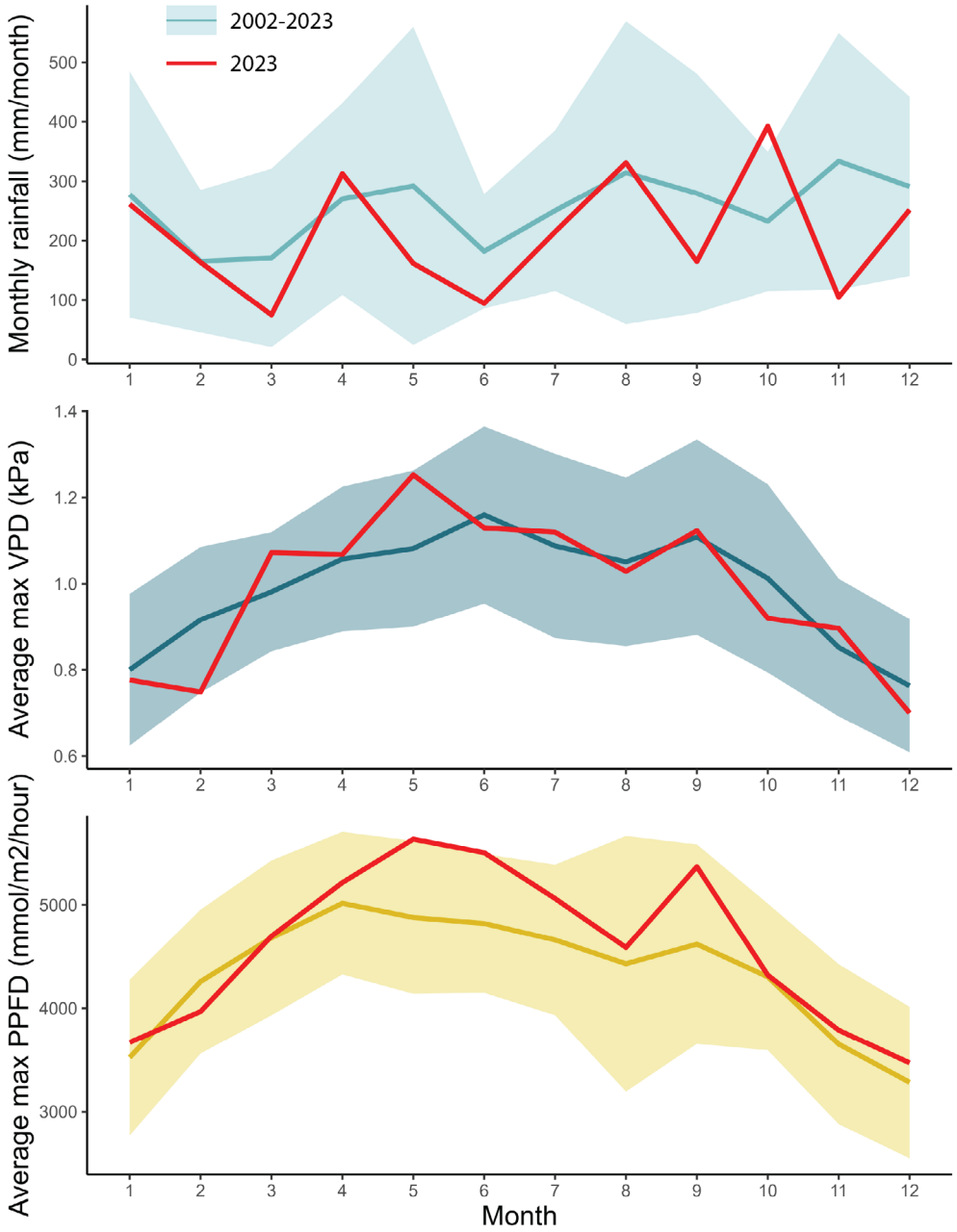

FIGURE 1 | Monthly climate summaries from 2002 to 2023 recorded at the nearby El Verde research station. Panels show monthly averages of total rainfall (mm/month), average daily maximum VPD per month (kPa) and average daily maximum PPFD per month (mmol/m^2/h). Hourly measurements were first aggregated to daily values, and monthly means were then calculated across all years. The thick lines indicate the multi-year monthly means and the shaded areas represent the standard deviation. The red line indicates the climate in 2023, which was used as reference year for the climate scenarios.

were removed. Daily sapflow totals were calculated by summing hourly sapflow rates over each 24-h period.

2.2 | Radial Stem Growth Calculation

We checked and processed the raw dendrometer data to extract radial growth using the *treenetproc* package (Knüsel et al. 2021). Data losses, primarily due to cable damage, and errors related to corrosion on springs were identified and addressed. We removed periods when the spring was stuck and the characteristic diurnal cycle was absent. Additionally, we excluded data showing large, abrupt jumps, which likely resulted from external disturbances (e.g., contact with a leaf, branch, or person). In such cases, we realigned the post-jump data so that the time series continued, minimizing the impact of these anomalies on our analyses. As a result, not all trees were represented for the full study duration (see Figure S3 for the start and end dates per tree).

Hourly stem dynamics were then translated to growth using a zero-growth model, which identifies stem size increases as growth only when the tree reaches a new maximum diameter (Zweifel et al. 2016) (Figure 2a & Figure S2). The average number of valid observation days per tree was 537 (SD ±167 days),

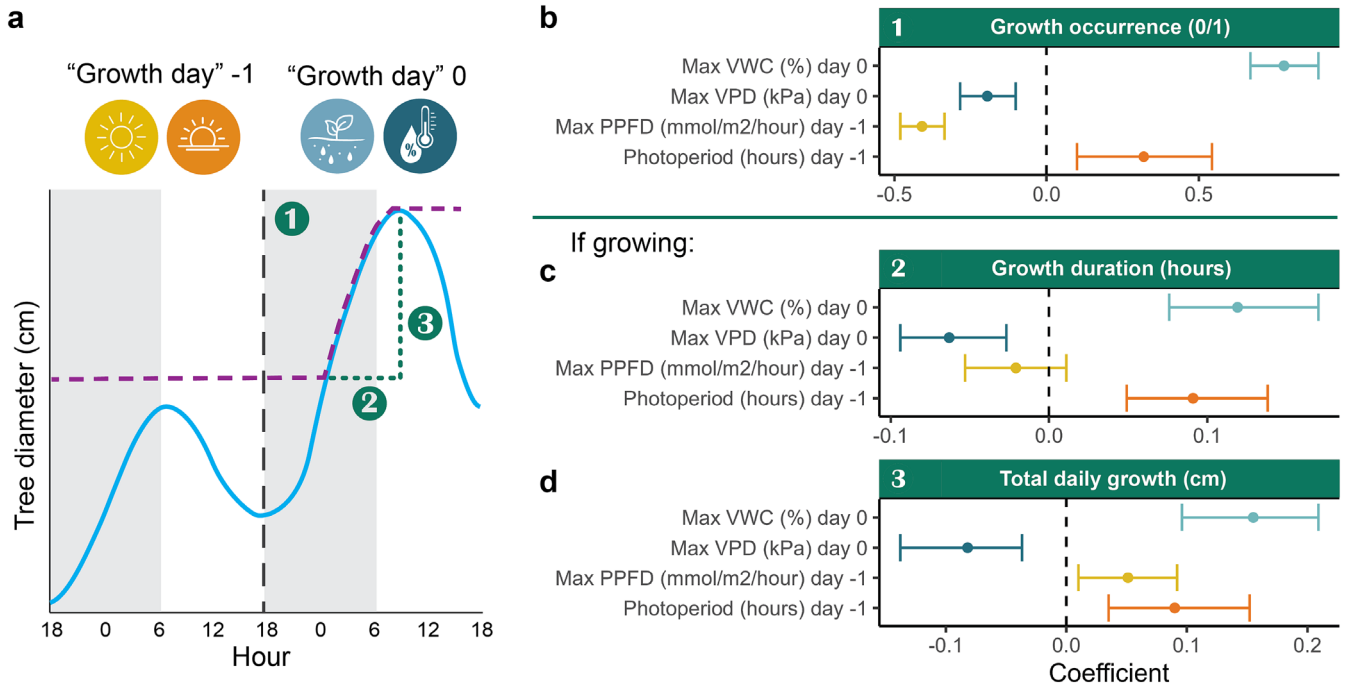

FIGURE 2 | Environmental drivers of stem growth responses across four tree species. (a) Schematic figure illustrating hourly growth data for two hypothetical growth days, alongside the three components of the model structure. The blue line represents stem size fluctuations due to expansion and shrinkage. The purple dotted line indicates the zero-growth model, which classifies stem size expansion as growth only when the tree reaches a new maximum diameter (Zweifel et al. 2016). Growth days are defined from 18 h until 18 h the following day, so as not to split overnight growth (gray shaded area) (Zweifel et al. 2021). Numbers correspond to the three processes in (b–d). (b–d) Model results are shown as posterior mean coefficients and 95% credible intervals for the effects of four environmental variables on three growth responses: (b) the probability of daily tree growth occurrence, (c) the growth duration per day (conditional on growth occurrence, hours); and (d) total daily growth (conditional on growth occurrence, cm). Predictor variables include current day ('growth day 0') maximum soil volumetric water content (VWC, %) and maximum vapor pressure deficit (VPD, kPa), combined with previous day ('growth day −1') maximum photosynthetically active radiation (PPFD, mmol/m^2/h) and photoperiod (hours of daylight). Coefficients and 95% credible intervals were estimated using 1000 draws from the posterior predictive distribution of a Bayesian joint model (Supporting Information S1). Colors indicate different predictor variables and correspond to icons in (a). Species responses can differ from the overall response, as indicated in Figures 3–5.

with values ranging from 100 to the full time period of 709 days. We defined a 'growth-day' as the 24-h period between 18:00 and 18:00 the next day, aligning with evidence that radial stem growth typically occurs at night (Figure S2c) (Zhou et al. 2023; Zweifel et al. 2021). For each growth-day, we quantified (1) whether growth occurred (binary), (2) the growth duration, or the number of hours during which growth was observed if growing, and (3) the total absolute radial growth that day (radial stem growth, cm). We compared our measured growth with long-term data from the adjacent LFDP, where individual trees are measured every 5 years, and confirmed that our estimates of growth fall within the ranges of average annual growth of the species (Figure S6).

2.3 | Statistical Analysis

We calculated the predictor variables maximum soil moisture (VWC, %) and vapor pressure deficit (VPD, kPa) for the growth-day itself (day 0) as these reflect the water availability during periods of growth (Zhou et al. 2023; Zweifel et al. 2016; Steppe et al. 2015). Maximum VPD was also calculated for the preceding growth-day (Peters, Kaewmano, et al. 2023). Additionally, maximum radiation and photoperiod were calculated for the previous growth-day (day −1), representing the amount of light potentially used for photosynthesis and carbon fixation (Steppe et al. 2015). This approach does not explicitly account for longer-term buildup of non-structural carbohydrates, which may allow for growth when circumstances are temporarily favorable. However, if carbohydrate storage plays an important role in these trees, we expect its influence to be partially captured by photoperiod as both fluctuate over the year with a longer photoperiod in the summer months when irradiance is higher, which could lead to higher storage of carbohydrates. We focused on daily maxima for each variable because trees often respond more strongly to extreme values than to means (Bauman et al. 2022). To assess the sensitivity of our results to this choice, we fitted an alternative model using daily mean values (see end of methods and Figure S10).

Pairwise correlations showed that none of the predictor variables were strongly correlated ($r < 0.52$), allowing them to be safely included in the model (Dormann et al. 2013). The exception was the correlation between maximum VPD and radiation on the same day (R^2 of 0.76, Figure S5). To test the influence of this relationship, we substituted radiation with VPD in an alternative model (Figure S8).

To evaluate the effects of environmental variables on radial stem growth, we developed a Bayesian joint model with three

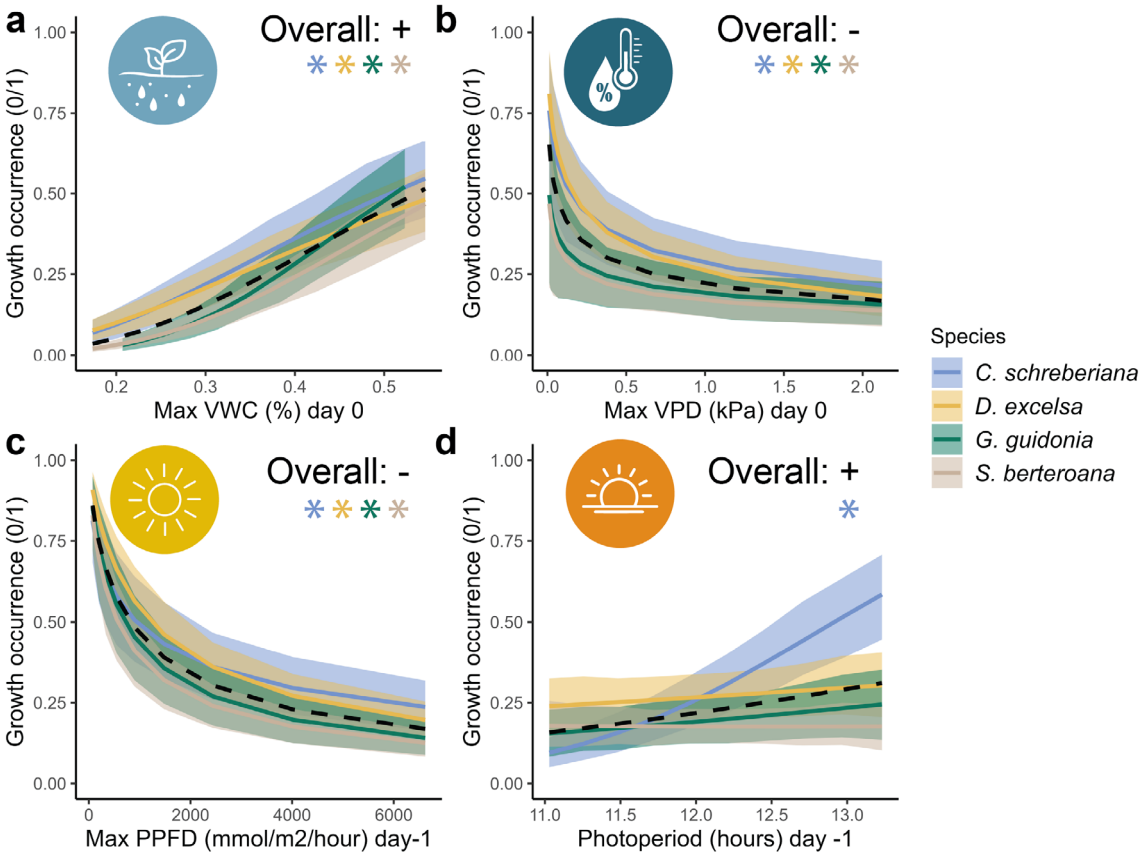

FIGURE 3 | Species level associations between environmental variables and the probability of growth occurrence. Panels show modeled relationships between the probability of observing growth (y-axes) and four environmental predictors (x-axes): (a) maximum soil volumetric water content (VWC, %), (b) maximum vapor pressure deficit (VPD, kPa), (c) previous day maximum active photosynthetic radiation (PPFD, mmol/m^2/h) and (d) previous day photoperiod day (hours of daylight). The black dotted lines denote the predicted mean across all four species; colored lines represent the species-specific mean predictions. Shaded regions indicate 95% credible intervals of these predictions, calculated from 1000 simulations of the posterior predictive distribution. Summary statistics are presented in each panel: Black symbols indicate overall model responses (+ for a positive association, − for a negative association, ns for not significant). Species-level estimates are marked with asterisks when significantly different from zero; responses in brackets indicate species-level effects with a direction different to the overall trend. A version of this figure including raw data is included as Figure S11.

components (see Supporting Information S1 for full model description and priors). The first component modeled the probability of growth for tree j of species l in plot k occurring during a particular day using a Bernoulli likelihood. The second component modeled the number of growth hours, conditional on growth occurrence, using a truncated negative binomial likelihood (excluding zeroes). The third component, with a Gamma likelihood, modeled total daily growth, also conditional on growth occurrence. All three components were modeled as a function of maximum VWC (*VWCmax*) and maximum VPD (*VPDmax*) and previous-day maximum PPFD (*PPFDmax*) and photoperiod (*DayLength*) (fixed effects).

We included species-level random slopes for each fixed effect, to allow species-level responses to deviate from the community-level mean (l). Additionally, we included random intercepts for each species (l), plot (k), and tree (j) across all three model components. The tree-level intercept (α_{tree}) was shared among components, capturing individual-level variation independent of covariates. Specifically, the tree level random intercepts for the second and the third component of the joint model shared the same hyperparameters as the tree-level intercept from the first component. These tree-level intercepts were multiplied by a scale parameter estimated from the data (Bauman et al. 2022), thus providing a link between the model estimating the probability of growth and the models estimating the number of growth hours or total growth per day. All predictor variables were log-transformed and standardized (z-scores) prior to analysis.

To account for temporal autocorrelation in the data, we incorporated an Ornstein-Uhlenbeck (OU) process, an alternative to auto-regressive type 1 (AR1) for continuous time series. We used the Integrated Nested Laplace Approximation (INLA) method (G'omez-Rubio 2020) for model fitting, chosen for its computational speed and its efficient handling of temporal autocorrelation. Model goodness-of-fit was assessed through posterior predictive checks based on 1000 simulations of the posterior predictive distribution (Figure S7).

2.4 | Alternative Model Variations

We tested the robustness of our conclusions by fitting three alternative models that retained the full joint structure. The first

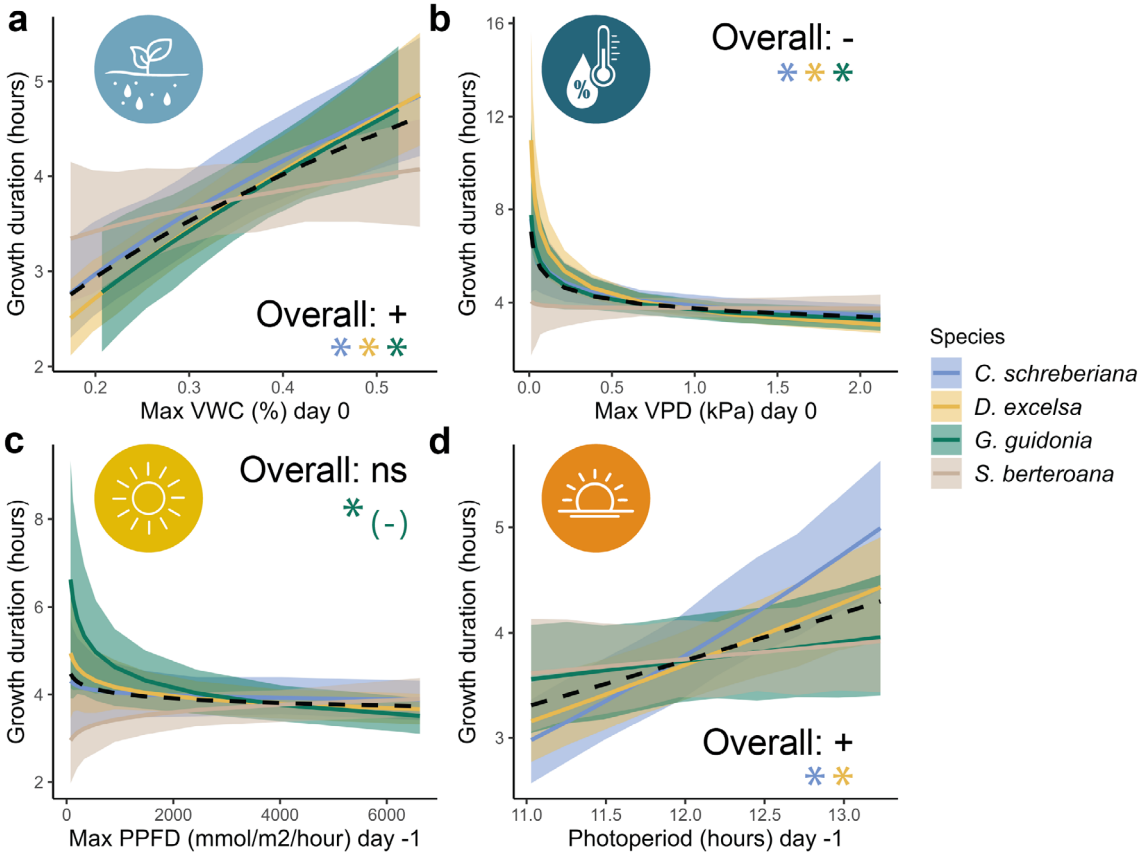

FIGURE 4 | Species level associations between environmental variables and growth duration. Panels show predicted growth duration (hours, y-axes) and four environmental predictors (x-axes): (a) maximum soil volumetric water content (VWC, %), (b) maximum vapor pressure deficit (VPD, kPa), (c) previous day maximum active photosynthetic radiation (PPFD, mmol/m^2/h), and (d) previous day photoperiod day (hours of daylight). The black dotted line represents the predicted mean across all four species; colored lines indicate species-specific mean predictions. Shaded regions represent 95% credible intervals of these predictions, calculated from 1000 simulations of the posterior predictive distribution. Summary statistics follow the convention established in Figure 3. A version of this figure including raw data is provided as Figure S12.

alternative model replaced previous day solar radiation with maximum VPD, given the high correlation between these variables (Figure S8). In this model, we found a positive association between previous-day VPD and total daily growth, which we interpreted as an indirect effect of solar radiation via evaporative demand.

Based on this result, we fitted a second alternative model, in which previous-day maximum VPD replaced solar radiation for the first two model components (growth occurrence and number of growth hours), while previous-day maximum PPFD was retained in the third component. This was motivated by the expectation that water limitation more strongly influences whether and how long trees grow, whereas total daily growth (when growth occurs) may be more driven by carbon assimilation from light availability. This model yielded results consistent with our original model (Figure S9): a negative effect of previous-day VPD on growth occurrence and only a minor positive effect of solar radiation on total daily growth.

A third alternative model used daily mean values for VWC, VPD, and radiation instead of their daily maxima to assess how averaging may influence observed associations with growth. This model reinforced the importance of water availability for growth occurrence (Figure S10), showing a positive association with soil moisture and a negative association with both previous-day VPD and radiation. However, in contrast to our main model, the third component revealed no relationship between soil moisture and total daily growth. As daily means may obscure short periods of (un)favorable growth conditions, especially under high variability, we concluded that daily maxima more accurately capture conditions under which growth occurs.

2.5 | Annual Growth for Four Climate Scenarios

We used the 1000 posterior samples from the main model to project annual radial stem growth for an individual of average size of each species under various climate scenarios. For the baseline prediction, we calculated daily growth using observed 2023 climate data, which was representative for climate conditions of the past 20 years (Figure 1), and species-specific model coefficients (the 'no-change' scenario). To simulate potential changes in climate conditions, we modified the 2023 environmental variables in several ways:

Scenario 1. Mean climate shift. Each daily environmental variable was uniformly adjusted by a fixed amount to reflect potential mean conditions. Regional projections consistently indicate reduced rainfall and higher temperatures (Miller and

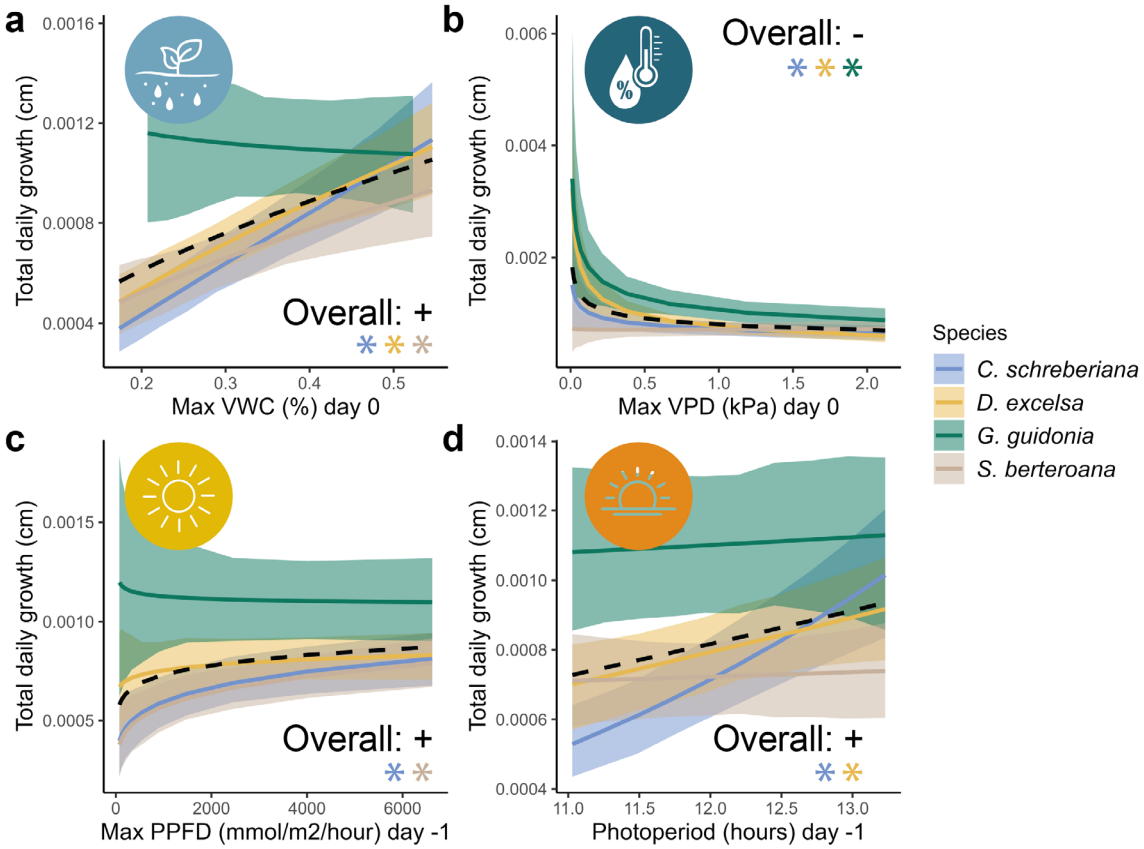

FIGURE 5 | Species level associations between environmental variables and total daily radial stem growth. Panels show modeled relationships between predicted daily growth (cm, y-axes) and four environmental predictors (x-axes): (a) maximum soil volumetric water content (VWC, %), (b) maximum vapor pressure deficit (VPD, kPa), (c) previous day maximum active photosynthetic radiation (PPFD, mmol/m^2/h) and (d) previous day photoperiod day (hours of daylight). The black dotted line indicates the predicted mean across all species, while colored lines represent species-specific mean responses. Shaded regions denote 95% credible intervals of these predictions, calculated from 1000 simulations of the posterior predictive distribution. Summary statistics follow the convention established in Figure 3. A version of this figure including raw data is provided as Figure S13.

Ramseyer 2024; IPCC 2021). Therefore, we tested the impact of higher VPD and PPFD, and lower VWC on tree growth. To define the magnitude of these adjustments, we used the severe drought of 2015 as an empirical benchmark rather than a specific future projected climate year. Using an observed event provides a well-constrained, internally consistent set of co-occurring climate variables that can plausibly happen in the near future, avoiding the additional uncertainty introduced by climate model spread and downscaling assumptions (Herrera and Ault 2017). The 2015 drought was the strongest in the past five decades, during which rainfall dropped to just 15%–25% of the long-term average (Smith-Martin et al. 2023; Guti'errez-Fonseca et al. 2020), making it a realistic upper bound for near-future drought conditions. Under this scenario, maximum VPD was increased by +0.5 kPa, maximum VWC decreased by 10%, and maximum PPFD increased by +1000 mmol m^{-2} h^{-1}. While we lack long-term soil moisture data in our plots, short dry periods in our dataset showed 10%–20% VWC reductions, rarely falling below 10% VWC; we thus applied a 10% VWC reduction but capped minimum values at 10%. Although no strong change in short-wave radiation was observed during the 2015 drought itself, we added 1000 mmol m^{-2} h^{-1} to simulate conditions where increased PPFD coincides with drought, equivalent to a 15%–50% rise in total daily PPFD.

Scenario 2. Combined drought effects. This scenario included simultaneous changes in VPD, VWC, and PPFD to reflect the compound nature of drought impacts on tree physiology. We applied the same increases and reductions as in scenario 1.

Scenario 3. Intensified extremes. Based on an analysis of historical climate data showing a 14% increase in days with VPD > 1 from 2012 to 2023 compared to 1999 to 2011 (despite no trend in mean VPD), we increased maximum VPD by +0.5 kPa to all days where it originally exceeded 0.7 kPa. On days with VWC below 23%, we subtracted an additional 10% to intensify the dry days without altering the wet conditions.

Scenario 4. Seasonal drought. We simulated seasonally targeted climate stress by only changing climate in the wetter, low VPD months (Dec–Feb) and sunniest/high VPD months (Jun–Aug). In those periods, we applied simultaneous increases in maximum VPD (+0.5 kPa), decreases in maximum VWC (−10%), and increased maximum PPFD (+1000 mmol/m^2/h) while leaving the rest of the year unchanged.

For each model and climate scenario, we calculated daily growth per species, which was aggregated to total annual growth. We derived mean annual growth and 95% credible

intervals from the 1000 model simulations using the highest posterior density intervals and compared them to baseline projections from 2023 to estimate percent change in growth. All statistical analyses were conducted in R Software (R Core Team 2024).

3 | Results

We observed high variability in radial stem growth among individuals during the study period. Some trees grew nearly continuously across all months, while others exhibited marked seasonality with pauses between bursts of growth (Figure S3). On days when growth occurred, trees grew from 1 to 22 h, with an average of 5.3 (±3.9 SD) hours, with growth happening mainly but not exclusively at night through early morning. Daily growth rates varied between 0.00038 and 0.21 mm per day, with a mean of 0.01 (±0.001 SD) mm/day.

3.1 | Water Sets the Stage for Radial Growth

We found water availability to be the most robust positive predictor of all three processes of radial stem growth across our four study species (Figures 2, 3–5a,b; see Supporting Information for the mathematical representation of the model). Higher soil VWC and lower atmospheric VPD were significantly associated with (i) a greater probability of growth occurrence (Figures 2b and 3), (ii) more hours of growth per day (Figures 2c and 4), and (iii) greater total daily growth (Figures 2d and 5). Light the previous day only became a significant positive driver for growth when growth was already underway (growth occurrence = 1): total daily growth was positively associated with higher PPFD (Figure 2d), but the effect size was still smaller than those of VWC and VPD.

Independent of total PPFD, we also found a consistent positive association between photoperiod and radial stem growth in all three modeled growth components (Figure 2). To ensure that the effect we attributed to photoperiod was not a side effect of overall higher PPFD in summer months, potentially leading to sugar buildup for use when water becomes available, we ran additional versions of the main model running over longer timescales. Although photoperiod was strongly correlated with both weekly ($r = 0.71$, $p < 0.001$) and monthly ($r = 0.85$, $p < 0.001$) summed PPFD, the model including photoperiod still outperformed both alternatives (lowest DIC and WAIC values), supporting the conclusion that photoperiod influences growth independently of concurrent increases in irradiance between May and July.

3.2 | Species-Specific Climate Sensitivity

The four species included in this study represent diverse life-history strategies, with an early (*Cecropia schreberiana*) (Brokaw 1998), a mid (*Guarea guidonia*) (Briscoe and Wadsworth 1970) and two late successional species (*Dacryodes excelsa* and *Sloanea berteroana*) (Briscoe and Wadsworth 1970). However, even with their different traits, differences in growth occurrence were limited (Figure 3). All species showed negative associations with drought-related variables (VWC, VPD) and previous-day PPFD, suggesting a shared sensitivity to water stress.

The main species difference was that the positive association between growth occurrence and photoperiod was significant only for *C. schreberiana* (Figure 3d). Other species exhibited more subtle differences. Among the four species, *S. berteroana* was the least responsive to environmental variation: the number of growth hours was not significantly associated with any of the tested environmental variables (Figure 4a–d). Furthermore, this species shared a slight positive response with increased PPFD on the previous day with the pioneer *C. schreberiana* (Figure 5c), potentially due to reduced sensitivity to VPD. Growth of *D. excelsa*, the dominant canopy tree in this forest (Thompson et al. 2002; Briscoe and Wadsworth 1970), was consistently negatively affected by water stress (Figures 4a,b and 5a,b) but benefited from longer day lengths (Figure 5d). *G. guidonia*, the mid-successional species, exhibited a different pattern: growth duration was strongly influenced by water and light availability (Figure 4a–c) but these effects were less pronounced for total daily growth (Figure 5a–c). Notably, *G. guidonia* also displayed the largest credible intervals in total daily growth, indicating substantial inter-individual variation in growth responses within the species (Figure 5).

3.3 | Growth and Climate Extremes

To further investigate the climate-growth relationship, we modeled total annual radial growth under a range of climate change scenarios (Figure 6). Our goal was not to predict long-term future forest-level growth responses per se, but rather to explore how plausible changes in climate and the timing of droughts could affect radial stem growth in these species. Of the individual environmental variables tested, reduced soil moisture (VWC) had the strongest negative effect on modeled annual radial stem growth across species (Figure 6, Scenario 1 'Mean shift'). However, the largest growth declines occurred when multiple variables were altered simultaneously to simulate compound drought conditions (Scenario 2 'Combined effects'). These results highlight the vulnerability of this forest community to the projected combination of rising temperatures and reduced rainfall.

To explore how increasing environmental variability influences growth independently of changes in annual means, we simulated a scenario in which only the driest days became more extreme while mean conditions remained stable (Scenario 3 'Intensified extremes'). This is consistent with an observed trend at the study site: the frequency of days with VPD > 1 kPa increased by 14% between 2012 and 2023 compared to 1999 and 2011, despite no change in mean VPD. Under this scenario, however, modeled radial stem growth remained largely unaffected.

We further tested whether the seasonal timing of drought mattered for annual growth outcomes (Scenario 4 'Seasonal drought'), by applying drought conditions either during the wetter, low-VPD months (December–February) or the typically drier, high-VPD months (June–August). Growth declines were most pronounced when drought occurred during the wetter

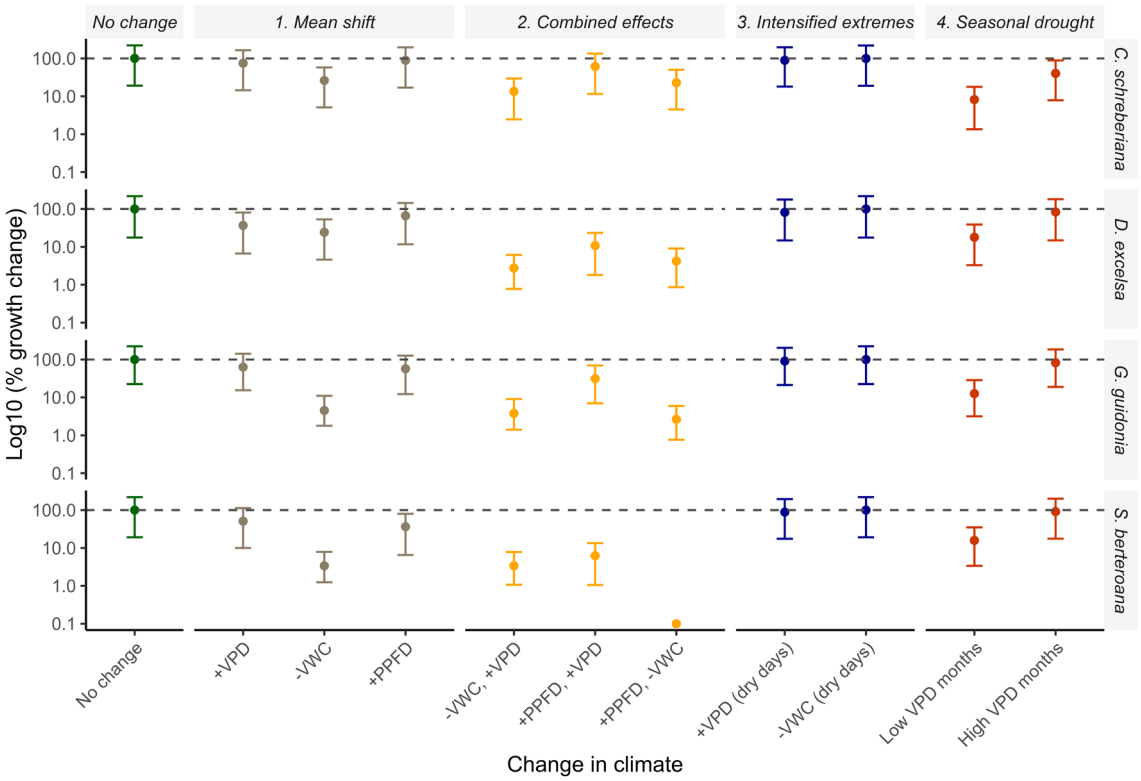

FIGURE 6 | Changes in annual growth per species under simulated climate scenarios. Total annual growth was calculated using 1000 simulated model coefficients under four climate scenarios, with observed 2023 climate conditions as the baseline. Each point shows the mean predicted change in growth for a given species under variations of one of four climate scenarios, expressed relative to 2023. Error bars indicate the 95% credible intervals. Note the log-scaled y-axis to better show differences between scenarios. Panels show the scenarios: No change, 1. Mean climate shift, 2. Combined drought effects, 3. Intensified extremes, with drier conditions on already dry days and 4. Seasonal droughts, in the months with low VPD (wetter; Dec–Feb) and high VPD and PPFD (drier; Jun–Aug). PPFD, photosynthetic photon flux density; VPD, maximum vapor pressure deficit; VWC, maximum soil volumetric water content.

months. The exception was *C. schreberiana*, a fast-growing pioneer with relatively consistent year-round growth, which also showed notable reductions under a summer drought.

4 | Discussion

Our findings challenge the prevailing paradigm that radial stem growth in everwet tropical forests is predominantly light-limited. Instead, we demonstrate that water availability, mediated through both soil moisture and VPD (Bauman et al. 2022), was the more critical driver. This pattern was consistent across four species with contrasting life-history strategies, even after accounting for random effects at both the plot and individual levels, suggesting a broad physiological constraint at this site. Our findings provide support for a working hypothesis that climate directly regulates growth in tropical forests, independent of its effects on photosynthesis. This implies that growth may be limited by sink capacity as well as by carbon supply. Whereas previous studies had documented this phenomenon in regions with distinct dry seasons and annual rainfall below 2000 mm (Peters, Kaewmano, et al. 2023; Zhou et al. 2023; Luse Belanganayi et al. 2024; Kaewmano et al. 2022), our results now show this in an everwet tropical forest with an annual rainfall of 3500 mm and no month with less than 100 mm of precipitation: a forest where water limitation on stem growth was not expected. We anticipate that rising temperatures and more frequent droughts will intensify drought stress in tropical forests by simultaneously depleting soil moisture and increasing atmospheric demand (VPD), constraining growth more than photosynthesis (Peters, Steppe, et al. 2023). Collectively, our findings support a growing body of evidence calling for the explicit integration of sink-limited, climate-driven growth into vegetation and Earth System Models (Peters, Kaewmano, et al. 2023; Fatichi et al. 2019; Xu et al. 2024). Incorporating such mechanisms is critical for improving projections of tropical forest carbon dynamics under future climate conditions.

4.1 | Water Over Light-Limited Growth

Our Bayesian joint model showed that even short periods of low water availability and/or increased VPD can suppress radial stem growth (Peters, Kaewmano, et al. 2023; Luse Belanganayi et al. 2024; Uriarte et al. 2016; Green 2024; Hofhansl et al. 2014). Observing water limitations on tree growth in such a wet forest is both unexpected and important, underscoring the need to reconsider how growth is incorporated into climate models (Fatichi et al. 2019; Restrepo-Coupe et al. 2017; Eckes-Shephard et al. 2021). In particular, our results challenge the assumption that increased GPP driven by elevated radiation automatically

enhances radial growth (Yang et al. 2023; Cernusak 2020; Ruehr et al. 2023; Zuidema et al. 2020). Trees were, in fact, significantly less likely to grow during nights following high-radiation days.

The reduced growth occurrence after a day with high PPFD coinciding with lower water availability and higher VPD could be attributed to various potential mechanisms: (i) water stress-induced limitations on photosynthesis from the previous day, resulting in decreased growth potential. However, we deem this is unlikely given the consistently high total sapflow of these trees at days with a higher VPD (but see the Section 4.4); (ii) higher investment in maintenance, roots or defense metabolism during the days with high PPFD, leaving less carbon for growth (Girardin et al. 2014); or (iii) a direct impact of water deficit on stem turgor pressure, negatively affecting growth (Peters, Kaewmano, et al. 2023; Anderegg et al. 2015). We consider the last hypothesis the most likely because on days when growth was already underway and water was therefore not limiting, prior-day radiation did have a small positive effect on total growth, indicating that high PPFD does not inherently suppress growth but requires adequate water availability to lead to growth. This interpretation was further supported by an alternative model substituting prior-day radiation with prior-day VPD, which confirmed a strong negative association between VPD and both growth occurrence and total growth. These results support an alternative working hypothesis that growth in this everwet forest is constrained not only by carbon supply (source limitation) but by the capacity to allocate that carbon to growth (sink limitation) (Cabon et al. 2022), consistent with growing evidence for a decoupling of productivity and radial stem growth across forest ecosystems (Friend et al. 2019; Wagner et al. 2016; Körner 2015).

4.2 | A Positive Association of Radial Growth With Photoperiod

Independent of total PPFD, we found a consistent positive association between photoperiod and all three modeled growth components, consistent with the few existing studies in subtropical forests accounting for this variable (Bosio et al. 2016; Shimamoto et al. 2016). Photoperiod differs from total PPFD in that it is determined solely by the duration of daylight (varying by approximately 2 h across the year at this site), independent of actual irradiance. A longer photoperiod may therefore represent a larger window for photosynthesis, potentially enhancing GPP and carbon availability for growth provided trees are not water stressed. In this way, photoperiod may define a seasonal window of opportunity for radial stem growth (Etzold et al. 2022), where growth occurrence, duration, and magnitude are greater during long, cloudy days than shorter, sunnier ones. Alternatively, these trees may exhibit a genetically programmed seasonal growth cycle, as photoperiod modulates the circadian clock and governs phenological transitions (Etzold et al. 2022; Roeber et al. 2021; Ding et al. 2021). However, the mechanistic basis of this effect remains uncertain. Photoperiod-driven growth regulation is predominantly documented in temperate and boreal species (Etzold et al. 2022; Ding et al. 2021), and photoperiod may act as a proxy for other unmeasured seasonal factors. Regardless of the mechanism, our findings highlight the importance of separating photoperiod and PPFD in seasonal growth analyses: conflating them risks misattributing seasonal growth increases to irradiance alone (Hogan et al. 2019).

4.3 | Implications for Growth Under Climate Change

Regional climate change projections indicate higher mean temperatures, reduced annual rainfall, and more frequent heat and drought extremes, with the strongest precipitation declines expected during the already high-VPD months of June to September (Miller and Ramseyer 2024; Almazroui et al. 2021; Bhardwaj et al. 2018). These changes will likely intensify drought stress by simultaneously depleting soil moisture and increasing atmospheric demand, constraining growth more than photosynthesis (Peters, Steppe, et al. 2023). However, if the extremes indeed intensify primarily during the dryer months when growth is already minimal, the impact on total annual growth may be limited (Niessner et al. 2020). If they fall during the wetter part of the year, the impact on growth will be more severe.

Because of the contrasting life histories and hydraulic traits of the studied species (Smith-Martin et al. 2023), we expected species-specific variation in responses to climate (Bauman et al. 2022). However, differences in growth occurrence were limited. All species showed negative associations with drought-related variables (VWC, VPD) and PPFD, suggesting a shared sensitivity to water stress, resulting in similar responses to the climate change scenarios. Growth of *D. excelsa*, the dominant canopy tree in this forest (Thompson et al. 2002; Briscoe and Wadsworth 1970), was consistently negatively affected by water stress. This response supports previous findings showing drought-induced growth reductions in *D. excelsa* during a severe drought (Smith-Martin et al. 2023). As this species accounts for approximately 16% of the basal area in this forest (Smith-Martin et al. 2023), its growth sensitivity to water availability has important implications for forest carbon dynamics and resilience under climate change.

The early-successional species *C. schreberiana* was the only species with a positive association between photoperiod and growth occurrence, growth duration, and total daily growth. This pattern may reflect its high maximum rate of net photosynthesis (Wen et al. 2008; Brokaw 1998) and flat, umbrella-shaped crown structure that allows most leaves to receive full sunlight. Together, these traits likely enable this species to take greater advantage of the extended daylight hours, particularly when water is not limiting, by sustaining high photosynthetic rates and supporting stem growth during longer photoperiods. However, it also showed a strong dependency on both soil moisture and VPD, indicating it will likely suffer under a dryer, hotter climate.

4.4 | Limitations and Future Perspectives

In this study, we set out to identify the climate variables most important for daily stem growth. However, without direct measurements of leaf-level photosynthesis and carbon allocation, we cannot empirically distinguish between carbon- and water-limited growth, and we therefore present this as a working

hypothesis. Trees could be preferentially allocating carbon to their roots or defense metabolism under dry conditions, for example, which would not be captured in our study. Nonetheless, several lines of indirect evidence suggest that carbon supply was not strongly limiting during the study period. Predawn water potentials confirmed trees were unstressed overnight (species averages: −0.27 to −0.37 MPa), sapflow remained high even on the driest days, suggesting stomatal conductance and photosynthetic potential were maintained (Lapa et al. 2017), and site VPD rarely exceeded 2 kPa, a threshold below which photosynthetic depression is limited (Slot et al. 2024). Weather conditions throughout the study period closely reflected long-term site averages, with no extreme drought or anomalous rainfall that might otherwise alter photosynthate allocation (Catovsky et al. 2002). Future work should prioritize direct physiological measurements such as in situ leaf photosynthesis, NSC sampling across tissues, and cambial activity via microcores or anatomical sections, to empirically distinguish water-driven turgor limitation from constraints on carbon supply.

A related open question concerns CO_2 fertilization. While elevated CO_2 has been shown to increase photosynthesis, it has not consistently translated into higher radial stem growth in tropical trees (Zuidema et al. 2020; Van der Sleen et al. 2015), but it did impact the sensitivity of tropical tree growth to climate (Zuidema et al. 2020). Our dataset is too short to test whether rising CO_2 could offset water deficits, so this remains an important avenue for future work in testing how these trees may respond to drought stress in the future.

Furthermore, our findings are based on 2 years of data from 35 trees across four species at a single site, which may limit their generalizability to a broader set of species or conditions. Additionally, the dataset spans only 2 years and therefore did not capture responses to rare or extreme climatic events such as severe drought. Nevertheless, we believe our study offers novel insights into water-growth relationships for several reasons. First, the four species capture variation in life history strategies, which is reflective of other wet tropical forests (Kambach et al. 2022). Second, average mean annual precipitation at our site is 3500 mm with no month receiving less than 100 mm of rainfall, while most studies linking water stress to tree demography have been conducted in more seasonal forests (Zuidema et al. 2022). The strength of the water-growth relationship likely varies among tropical forests depending on local factors such as soil type (Zhou et al. 2023; Kaewmano et al. 2022), highlighting the need for a broader range of studies. It would be valuable to expand this dataset further by connecting to existing tropical forest networks such as ForestGEO or ForestPlots.NET to determine the generality of our results and link them to long-term growth trends.

Finally, the zero-growth model assumes that no cambial activity occurs during stem shrinkage, potentially leading to an underestimation of growth during water stress periods when true expansion is masked by elastic shrinkage. Complementary approaches including process-based growth modelling (Peters, Kaewmano, et al. 2023), advanced data processing methods (Liu et al. 2025; Mencuccini et al. 2017; Chan et al. 2016), and high-resolution anatomical techniques such as cambial pinning (Trouet et al. 2012) and microcores (Luse Belanganayi et al. 2025), would help disentangle water flux signals from growth and further clarify the timing and drivers of cambial activity in these everwet ecosystems. Together, these limitations highlight that while our findings robustly identified water availability as the dominant short-term constraint on stem growth, the longer-term interplay between carbon source dynamics, sink activity, and organ-level allocation remains an important avenue for future research in everwet tropical forests.

Author Contributions

Chris M. Smith-Martin: conceptualization, investigation, funding acquisition, methodology, writing – review and editing, project administration. **Tana E. Wood:** conceptualization, investigation, funding acquisition, writing – review and editing, supervision. **Jess K. Zimmerman:** conceptualization, investigation, funding acquisition, writing – review and editing, supervision, project administration. **María Uriarte:** conceptualization, funding acquisition, investigation, writing – review and editing, methodology, formal analysis, project administration, supervision. **Laura E. Boeschoten:** conceptualization, investigation, writing – original draft, methodology, visualization, writing – review and editing, formal analysis, data curation. **Jose A. Medina-Vega:** formal analysis, writing – review and editing. **Monique Picón:** project administration, data curation, investigation. **Mukund P. Rao:** writing – review and editing, conceptualization, data curation, methodology. **Luis A. Esbrí Ruiz:** data curation, investigation. **Rebecca A. Montgomery:** conceptualization, investigation, funding acquisition, writing – review and editing, supervision. **Kristina J. Anderson-Teixeira:** conceptualization, writing – review and editing, investigation. **Xiangtao Xu:** conceptualization, investigation, funding acquisition, writing – review and editing, supervision.

Acknowledgments

This work was supported by US National Science Foundation (NSF-DEB) grant 2140580 to M.U., R.A.M., C.S.M., T.E.W, and X.X. The tree census data was collected through NSF award numbers 1831952 and 2425484. L.E.B. also acknowledges the 2024 ForestGEO workshop during which the paper received a strong push towards publication. M.P.R. acknowledges support from the Vetlesen Foundation and EU Horizon 2020 Marie Sklodowska-Curie grant TERRACARB #101031748. X.X. acknowledges support from U.S. Department of Energy Environmental System Science Program grant DE-SC0023048.

Funding

This work was supported by the National Science Foundation (2140580), H2020 Marie Skłodowska-Curie Actions (TERRACARB #101031748), and U.S. Department of Energy (DE-SC0023048).

Conflicts of Interest

The authors declare no conflicts of interest.

Data Availability Statement

The data that support the findings of this study are openly available in Zenodo at https://doi.org/10.5281/zenodo.19187657. Additionally, climate data for the site are available at the EDI data portal from: https://portal.edirepository.org/nis/mapbrowse?scope=knb-lter-luqidentifier=127revision=1676181.

References

Almazroui, M., M. N. Islam, F. Saeed, et al. 2021. “Projected Changes in Temperature and Precipitation Over the United States, Central

America, and the Caribbean in CMIP6 GCMs." *Earth Systems and Environment* 5: 1–24.

Anderegg, W. R. L., A. P. Ballantyne, W. K. Smith, et al. 2015. "Tropical Nighttime Warming as a Dominant Driver of Variability in the Terrestrial Carbon Sink." *Proceedings of the National Academy of Sciences of the United States of America* 112: 15591–15596.

Anderson, L. O., G. Ribeiro Neto, A. P. Cunha, et al. 2018. "Vulnerability of Amazonian Forests to Repeated Droughts." *Philosophical Transactions of the Royal Society, B: Biological Sciences* 373: 20170411.

Anderson-Teixeira, K. J., V. Herrmann, R. Banbury Morgan, et al. 2021. "Carbon Cycling in Mature and Regrowth Forests Globally." *Environmental Research Letters* 16: 053009.

Angoboy Ilondea, B., H. Beeckman, J. van Acker, et al. 2021. "Variation in Onset of Leaf Unfolding and Wood Formation in a Central African Tropical Tree Species." *Frontiers in Forests and Global Change* 4: 673575.

Babst, F., A. D. Friend, M. Karamihalaki, et al. 2021. "Modeling Ambitions Outpace Observations of Forest Carbon Allocation." *Trends in Plant Science* 26: 210–219.

Bauman, D., C. Fortunel, G. Delhaye, et al. 2022. "Tropical Tree Mortality Has Increased With Rising Atmospheric Water Stress." *Nature* 608: 528–533.

Bhardwaj, A., V. Misra, A. Mishra, et al. 2018. "Downscaling Future Climate Change Projections Over Puerto Rico Using a Nonhydrostatic Atmospheric Model." *Climatic Change* 147: 133–147.

Bonan, G. B., and S. C. Doney. 2018. "Climate, Ecosystems, and Planetary Futures: The Challenge to Predict Life in Earth System Models." *Science* 359: eaam8328.

Bosio, F., S. Rossi, and C. R. Marcati. 2016. "Periodicity and Environmental Drivers of Apical and Lateral Growth in a Cerrado Woody Species." *Trees* 30: 1495–1505.

Briscoe, C. B., and F. H. Wadsworth. 1970. "Stand Structure and Yield in the Tabonuco Forest of Puerto Rico." In *A Tropical Rain Forest*, edited by H. T. Odum, B79–B89. Division of Technical Information, US Atomic Energy Commission.

Brokaw, N. V. L. 1998. "*Cecropia schreberiana* in the Luquillo Mountains of Puerto Rico." *Botanical Review* 64: 91–120.

Cabon, A., S. A. Kannenberg, A. Arain, et al. 2022. "Cross-Biome Synthesis of Source Versus Sink Limits to Tree Growth." *Science* 376: 758–761.

Canadell, J., P. M. S. Monteiro, M. H. Costa, et al. 2021. "Global Carbon and Other Biogeochemical Cycles and Feedbacks." In *Climate Change 2021 – The Physical Science Basis: Working Group I Contribution to the Sixth Assessment Report of the Intergovernmental Panel on Climate Change*, 1st ed., 673–816. Cambridge University Press. ISBN: 978-1-009-15789-6.

Catovsky, S., N. M. Holbrook, and F. A. Bazzaz. 2002. "Coupling Whole-Tree Transpiration and Canopy Photosynthesis in Coniferous and Broad-Leaved Tree Species." *Canadian Journal of Forest Research* 32: 295–309.

Cernusak, L. A. 2020. "Gas Exchange and Water-Use Efficiency in Plant Canopies." *Plant Biology* 22, no. S1: 52–67.

Chan, T., T. Hölttä, F. Berninger, et al. 2016. "Separating Water-Potential Induced Swelling and Shrinking From Measured Radial Stem Variations Reveals a Cambial Growth and Osmotic Concentration Signal." *Plant, Cell & Environment* 39: 233–244.

Clark, D. B., D. A. Clark, and S. F. Oberbauer. 2010. "Annual Wood Production in a Tropical Rain Forest in NE Costa Rica Linked to Climatic Variation but Not to Increasing CO2." *Global Change Biology* 16: 747–759.

Ding, J., B. Zhang, Y. Li, D. André, and O. Nilsson. 2021. "Phytochrome B and PHYTOCHROME INTERACTING FACTOR8 Modulate Seasonal Growth in Trees." *New Phytologist* 232: 2339–2352.

Dormann, C. F., J. Elith, S. Bacher, et al. 2013. "Collinearity: A Review of Methods to Deal With It and a Simulation Study Evaluating Their Performance." *Ecography* 36: 27–46.

Duursma, R. A. 2015. "Plantecophys—An R Package for Analysing and Modelling Leaf Gas Exchange Data." *PLoS One* 10: e0143346.

Eckes-Shephard, A. H., A. P. K. Argles, B. Brzeziecki, et al. 2025. "Demography, Dynamics and Data: Building Confidence for Simulating Changes in the World's Forests." *New Phytologist* 248: 2722–2749.

Eckes-Shephard, A. H., E. Tiavlovsky, Y. Chen, P. Fonti, and A. D. Friend. 2021. "Direct Response of Tree Growth to Soil Water and Its Implications for Terrestrial Carbon Cycle Modelling." *Global Change Biology* 27: 121–135.

Etzold, S., F. Sterck, A. K. Bose, et al. 2022. "Number of Growth Days and Not Length of the Growth Period Determines Radial Stem Growth of Temperate Trees." *Ecology Letters* 25: 427–439.

Ewel, J., and J. Whitmore. 1973. *The Ecological Life Zones of Puerto Rico and the US Virgin Islands*. USDA Forest Service.

Fang, Z., W. Zhang, M. Brandt, A. M. Abdi, and R. Fensholt. 2022. "Globally Increasing Atmospheric Aridity Over the 21st Century." *Earth's Future* 10: e2022EF003019.

Fatichi, S., S. Leuzinger, and C. Körner. 2014. "Moving Beyond Photosynthesis: From Carbon Source to Sink-Driven Vegetation Modeling." *New Phytologist* 201: 1086–1095.

Fatichi, S., C. Pappas, J. Zscheischler, and S. Leuzinger. 2019. "Modelling Carbon Sources and Sinks in Terrestrial Vegetation." *New Phytologist* 221: 652–668.

Feron, S., R. R. Cordero, A. Damiani, et al. 2024. "South America Is Becoming Warmer, Drier, and More Flammable." *Communications Earth & Environment* 5: 501.

Friend, A. D., A. H. Eckes-Shephard, P. Fonti, et al. 2019. "On the Need to Consider Wood Formation Processes in Global Vegetation Models and a Suggested Approach." *Annals of Forest Science* 76: 1–13.

Gessler, A., and R. Zweifel. 2024. "Beyond Source and Sink Control – Toward an Integrated Approach to Understand the Carbon Balance in Plants." *New Phytologist* 242: 858–869.

Gheyret, G., H.-T. Zhang, Y. Guo, et al. 2021. "Radial Growth Response of Trees to Seasonal Soil Humidity in a Subtropical Forest." *Basic and Applied Ecology* 55: 74–86.

Giraldo, J. A., J. I. del Valle, S. González-Caro, et al. 2023. "Tree Growth Periodicity in the Ever-Wet Tropical Forest of the Americas." *Journal of Ecology* 111: 889–902.

Girardin, C. A., J. E. Silva Espejob, C. E. Doughty, et al. 2014. "Productivity and Carbon Allocation in a Tropical Montane Cloud Forest in the Peruvian Andes." *Plant Ecology and Diversity* 7: 107–123.

G'omez-Rubio, V. 2020. *Bayesian Inference With INLA*. Chapman & Hall/CRC Press.

Graham, E. A., S. S. Mulkey, K. Kitajima, N. G. Phillips, and S. J. Wright. 2003. "Cloud Cover Limits Net CO_2 Uptake and Growth of a Rainforest Tree During Tropical Rainy Seasons." *Proceedings of the National Academy of Sciences of the United States of America* 100: 572–576.

Green, J. K. 2024. "The Intricacies of Vegetation Responses to Changing Moisture Conditions." *New Phytologist* 244: 2156–2162.

Green, J. K., J. Berry, P. Ciais, Y. Zhang, and P. Gentine. 2020. "Amazon Rainforest Photosynthesis Increases in Response to Atmospheric Dryness." *Science Advances* 6: eabb7232.

Grossiord, C., T. N. Buckley, L. A. Cernusak, et al. 2020. "Plant Responses to Rising Vapor Pressure Deficit." *New Phytologist* 226: 1550–1566.

Guti'errez-Fonseca, P. E., A. Ramírez, C. M. Pringle, et al. 2020. "When the Rainforest Dries: Drought Effects on a Montane Tropical Stream Ecosystem in Puerto Rico." *Freshwater Science* 39: 197–212.

Herrera, D., and T. Ault. 2017. "Insights From a New High-Resolution Drought Atlas for the Caribbean Spanning 1950–2016." *Journal of Climate* 30: 7801–7825.

Hofhansl, F., J. Kobler, J. Ofner, S. Drage, E. M. Pölz, and W. Wanek. 2014. "Sensitivity of Tropical Forest Aboveground Productivity to Climate Anomalies in SW Costa Rica." *Global Biogeochemical Cycles* 28: 1437–1454.

Hogan, J. A., S. M. McMahon, V. Buzzard, et al. 2019. "Drought and the Interannual Variability of Stem Growth in an Aseasonal, Everwet Forest." *Biotropica* 51: 139–154.

Hubau, W., S. L. Lewis, O. L. Phillips, et al. 2020. "Asynchronous Carbon Sink Saturation in African and Amazonian Tropical Forests." *Nature* 579: 80–87.

Huke, R. E. 1982. *Agroclimatic and Dry-Season Maps of South, Southeast, and East Asia*. International Rice Research Institute.

IPCC. 2021. "Weather and Climate Extreme Events in a Changing Climate." In *Climate Change 2021 – The Physical Science Basis: Working Group I Contribution to the Sixth Assessment Report of the Intergovernmental Panel on Climate Change*, 1513–1766. Cambridge University Press. ISBN: 978-1-009-15788-9.

Kaewmano, A., P. L. Fu, Z. X. Fan, N. Pumijumnong, P. A. Zuidema, and A. Bräuning. 2022. "Climatic Influences on Intra-Annual Stem Radial Variations and Xylem Formation of *Toona ciliata* at Two Asian Tropical Forest Sites With Contrasting Soil Water Availability." *Agricultural and Forest Meteorology* 318: 108906.

Kambach, S., R. Condit, S. Aguilar, et al. 2022. "Consistency of Demographic Trade-Offs Across 13 (Sub)tropical Forests." *Journal of Ecology* 110: 1485–1496.

Keenan, T. F., I. C. Prentice, J. G. Canadell, et al. 2016. "Recent Pause in the Growth Rate of Atmospheric CO_2 due to Enhanced Terrestrial Carbon Uptake." *Nature Communications* 7: 13428.

Knauer, J., M. Cuntz, B. Smith, et al. 2023. "Higher Global Gross Primary Productivity Under Future Climate With More Advanced Representations of Photosynthesis." *Science Advances* 9: eadh9444.

Knüsel, S., R. L. Peters, M. Haeni, M. Wilhelm, and R. Zweifel. 2021. "Processing and Extraction of Seasonal Tree Physiological Parameters From Stem Radius Time Series." *Forests* 12: 765.

Körner, C. 2015. "Paradigm Shift in Plant Growth Control." *Current Opinion in Plant Biology* 25: 107–114.

Koven, C. D., R. G. Knox, R. A. Fisher, et al. 2020. "Benchmarking and Parameter Sensitivity of Physiological and Vegetation Dynamics Using the Functionally Assembled Terrestrial Ecosystem Simulator (FATES) at Barro Colorado Island, Panama." *Biogeosciences* 17: 3017–3044.

Lapa, G., F. Morandini, and L. Ferrat. 2017. "Sap Flow and Photosynthetic Response to Climate and Drought of *Pinus nigra* in a Mediterranean Natural Forest." *Trees* 31: 1711–1721.

Liu, C., M. Peltoniemi, P. Alekseychik, A. Mäkelä, and T. Hölttä. 2025. "A Coupled Model of Hydraulic EcoPhysiology and Cambial Growth—Accounting for Biophysical Limitations and Phenology Improves Stem Diameter Prediction at High Temporal Resolution." *Plant, Cell & Environment* 48: 1344–1365.

Luo, L.-X., Z.-Y. Sun, and Z.-H. Tan. 2024. "Climate Seasonality of Tropical Evergreen Forest Region." *Water* 16: 749.

Luse Belanganayi, B., B. A. Ilondea, C. M. Phaka, et al. 2024. "Diel and Annual Rhythms of Tropical Stem Size Changes in the Mayombe Forest, Congo Basin." *Frontiers in Forests and Global Change* 7: 1185225.

Luse Belanganayi, B., C. M. Phaka, B. Y. Djiofack, et al. 2025. "Timing of Cambial Phenology of Rainforest Trees as Indicator of Climate Sensitivity of the Congo Basin Biome." *Global Ecology and Conservation* 62: e03740.

Mencuccini, M., Y. Salmon, P. Mitchell, et al. 2017. "An Empirical Method That Separates Irreversible Stem Radial Growth From Bark Water Content Changes in Trees: Theory and Case Studies." *Plant, Cell & Environment* 40: 290–303.

Miller, P. W., and C. Ramseyer. 2024. "The Relationship Between the Saharan Air Layer, Convective Environmental Conditions, and Precipitation in Puerto Rico." *Journal of Geophysical Research: Atmospheres* 129: e2023JD039681.

Muller-Landau, H. C., K. C. Cushman, E. E. Arroyo, I. Martinez Cano, K. J. Anderson-Teixeira, and B. Backiel. 2021. "Patterns and Mechanisms of Spatial Variation in Tropical Forest Productivity, Woody Residence Time, and Biomass." *New Phytologist* 229: 3065–3087.

Niessner, A., M. Küppers, J. Graham, et al. 2020. "Climate and Seasonal Rainfall Anomalies Along an Elevational Gradient in the El Sira Mountains, Peru, and Their Impacts on Tree Radial Growth." *Journal of Forestry Research* 31: 1521–1538.

O'Connell, C. S., L. Ruan, and W. L. Silver. 2018. "Drought Drives Rapid Shifts in Tropical Rainforest Soil Biogeochemistry and Greenhouse Gas Emissions." *Nature Communications* 9: 1348.

Pan, Y., R. A. Birdsey, O. L. Phillips, et al. 2024. "The Enduring World Forest Carbon Sink." *Nature* 631: 563–569.

Peters, R. L., A. Kaewmano, P. L. Fu, et al. 2023. "High Vapour Pressure Deficit Enhances Turgor Limitation of Stem Growth in an Asian Tropical Rainforest Tree." *Plant, Cell & Environment* 46: 2747–2762.

Peters, R. L., K. Steppe, C. Pappas, et al. 2023. "Daytime Stomatal Regulation in Mature Temperate Trees Prioritizes Stem Rehydration at Night." *New Phytologist* 239: 533–546.

R Core Team. 2024. *R: A Language and Environment for Statistical Computing*. R version 4.4.1. R Foundation for Statistical Computing.

Restrepo-Coupe, N., H. R. da Rocha, L. R. Hutyra, et al. 2013. "What Drives the Seasonality of Photosynthesis Across the Amazon Basin? A Cross-Site Analysis of Eddy Flux Tower Measurements From the Brasil Flux Network." *Agricultural and Forest Meteorology* 182-183: 128–144.

Restrepo-Coupe, N., N. M. Levine, B. O. Christoffersen, et al. 2017. "Do Dynamic Global Vegetation Models Capture the Seasonality of Carbon Fluxes in the Amazon Basin? A Data-Model Intercomparison." *Global Change Biology* 23: 191–208.

Rifai, S. W., C. A. J. Girardin, E. Berenguer, et al. 2018. "ENSO Drives Interannual Variation of Forest Woody Growth Across the Tropics." *Philosophical Transactions of the Royal Society, B: Biological Sciences* 373: 20170410.

Roeber, V. M., I. Bajaj, M. Rohde, T. Schmülling, and A. Cortleven. 2021. "Light Acts as a Stressor and Influences Abiotic and Biotic Stress Responses in Plants." *Plant, Cell & Environment* 44: 645–664.

Ruehr, S., T. F. Keenan, C. Williams, et al. 2023. "Evidence and Attribution of the Enhanced Land Carbon Sink." *Nature Reviews Earth & Environment* 4: 518–534.

Scatena, F. 2001. "Ecological Rhythms and the Management of Humid Tropical Forests." *Forest Ecology and Management* 154: 453–464.

Shekhar, A., L. Hörtnagl, N. Buchmann, and M. Gharun. 2023. "Long-Term Changes in Forest Response to Extreme Atmospheric Dryness." *Global Change Biology* 29: 5379–5396.

Shimamoto, C. Y., P. C. Botosso, E. Amano, and M. C. M. Marques. 2016. "Stem Growth Rhythms in Trees of a Tropical Rainforest in Southern Brazil." *Trees* 30: 99–111.

Slot, M., S. W. Rifai, C. E. Eze, and K. Winter. 2024. "The Stomatal Response to Vapor Pressure Deficit Drives the Apparent Temperature Response of Photosynthesis in Tropical Forests." *New Phytologist* 244: 1238–1249.

Smith-Martin, C. M., R. Muscarella, R. Ankori-Karlinsky, et al. 2023. "Hydraulic Traits Are Not Robust Predictors of Tree Species Stem Growth During a Severe Drought in a Wet Tropical Forest." *Functional Ecology* 37: 447–460.

Spannl, S., F. Volland, D. Pucha, T. Peters, E. Cueva, and A. Bräuning. 2016. "Climate Variability, Tree Increment Patterns and ENSO-Related Carbon Sequestration Reduction of the Tropical Dry Forest Species Loxopterygium Huasango of Southern Ecuador." *Trees* 30: 1245–1258.

Steppe, K., F. Sterck, and A. Deslauriers. 2015. "Diel Growth Dynamics in Tree Stems: Linking Anatomy and Ecophysiology." *Trends in Plant Science* 20: 335–343.

Thompson, J., N. Brokaw, J. K. Zimmerman, et al. 2002. "Land Use History, Environment, and Tree Composition in A Tropical Forest." *Ecological Applications* 12: 1344–1363.

Trew, B. T., D. P. Edwards, A. C. Lees, et al. 2024. "Novel Temperatures Are Already Widespread Beneath the World's Tropical Forest Canopies." *Nature Climate Change* 14: 753–759.

Trouet, V., M. Mukelabai, A. Verheyden, and H. Beeckman. 2012. "Cambial Growth Season of Brevi-Deciduous *Brachystegia spiciformis* Trees From South Central Africa Restricted to Less Than Four Months." *PLoS One* 7: e47364.

Trugman, A. T., and L. D. L. Anderegg. 2025. "Source vs Sink Limitations on Tree Growth: From Physiological Mechanisms to Evolutionary Constraints and Terrestrial Carbon Cycle Implications." *New Phytologist* 245: 966–981.

Uriarte, M., J. R. Lasky, V. K. Boukili, and R. L. Chazdon. 2016. "A Trait-Mediated, Neighbourhood Approach to Quantify Climate Impacts on Successional Dynamics of Tropical Rainforests." *Functional Ecology* 30: 157–167.

Van der Sleen, P., P. Groenendijk, M. Vlam, et al. 2015. "No Growth Stimulation of Tropical Trees by 150 Years of CO_2 Fertilization but Water-Use Efficiency Increased." *Nature Geoscience* 8: 24–28.

van Schaik, C. P., J. W. Terborgh, and S. J. Wright. 1993. "The Phenology of Tropical Forests: Adaptive Significance and Consequences for Primary Consumers." *Annual Review of Ecology and Systematics* 24: 353–377.

Wagner, F. H., B. Hérault, D. Bonal, et al. 2016. "Climate Seasonality Limits Leaf Carbon Assimilation and Wood Productivity in Tropical Forests." *Biogeosciences* 13: 2537–2562.

Wagner, F., V. Rossi, M. Aubry-Kientz, et al. 2014. "Pan-Tropical Analysis of Climate Effects on Seasonal Tree Growth." *PLoS One* 9: e92337.

Wen, S., N. Fetcher, and J. K. Zimmerman. 2008. "Acclimation of Tropical Tree Species to Hurricane Disturbance: Ontogenetic Differences." *Tree Physiology* 28: 935–946.

Xu, X., D. Medvigy, J. S. Powers, J. M. Becknell, and K. Guan. 2016. "Diversity in Plant Hydraulic Traits Explains Seasonal and Inter-Annual Variations of Vegetation Dynamics in Seasonally Dry Tropical Forests." *New Phytologist* 212: 80–95.

Xu, X., P. van der Sleen, P. Groenendijk, et al. 2024. "Constraining Long-Term Model Predictions for Woody Growth Using Tropical Tree Rings." *Global Change Biology* 30: e17075.

Yaffar, D., and R. J. Norby. 2020. "A Historical and Comparative Review of 50 Years of Root Data Collection in Puerto Rico." *Biotropica* 52: 563–576.

Yang, L.-Y., R. Yu, J. Wu, et al. 2023. "Asian Tropical Forests Assimilating Carbon Under Dry Conditions: Water Stress or Light Benefits?" *Journal of Plant Ecology* 16: rtac106.

Zhou, B., F. Sterck, B. Kruijt, Z.-X. Fan, and P. A. Zuidema. 2023. "Diel and Seasonal Stem Growth Responses to Climatic Variation Are Consistent Across Species in a Subtropical Tree Community." *New Phytologist* 240: 2253–2264.

Zuidema, P. A., F. Babst, P. Groenendijk, et al. 2022. "Tropical Tree Growth Driven by Dry-Season Climate Variability." *Nature Geoscience* 15: 269–276.

Zuidema, P. A., I. Heinrich, M. Rahman, M. Vlam, S. A. Zwartsenberg, and P. Sleen. 2020. "Recent CO2 Rise Has Modified the Sensitivity of Tropical Tree Growth to Rainfall and Temperature." *Global Change Biology* 26: 4028–4041.

Zwartsenberg, S. A., F. J. Sterck, L. Haddad, et al. 2025. "Centennial-Scale Atmospheric CO_2 Rise Increased Photosynthetic Efficiency in a Tropical Tree Species." *New Phytologist* 246: 131–143.

Zweifel, R., M. Haeni, N. Buchmann, and W. Eugster. 2016. "Are Trees Able to Grow in Periods of Stem Shrinkage?" *New Phytologist* 211: 839–849.

Zweifel, R., F. Sterck, S. Braun, et al. 2021. "Why Trees Grow at Night." *New Phytologist* 231: 2174–2185.

Supporting Information

Additional supporting information can be found online in the Supporting Information section. **Figure S1:** Climatic representativeness of published studies on climate-growth relationships. Adapted from Zuidema et al. (2022): green background indicates the distribution of the tropical land area with woody vegetation. Open shapes represent study sites where chronologies have been developed and that are represented in the tropical tree ring network. We added published point dendrometer studies (purple, 1–7) and the one inter-annual census study in an area with over 3000 mm of annual rainfall (green, 8). Our study site is represented by the yellow dot, at 3500 mm rainfall and 25.2°C. **Figure S2:** Daily growth patterns and growth contribution per hour of the day. (a) Hourly VPD (black lines, kPa) and rainfall (blue bars, mm) across four days in July, 2023. (b) Radial stem growth dynamics example of two trees, one *C. schreberiana* (CECSCH) individual and one *D. excelsa* (DACEXC) individual on the same days. Solid lines depict the daily stem cycle. Dotted lines show the zero-growth model, indicating growth is only considered if the tree reaches a new maximum diameter. (c) Mean and standard deviations of hourly radial stem growth across the 24-h cycle, summarized for the four study species. Daily growth was calculated from 18:00 until 18:00 the next day to account for growth at night. **Figure S3:** Scaled stem diameter trajectories over the study period. The y-axis shows each tree's DBH, scaled between 0 and 1, the x-axes represent time. DBH values reflect the maximum stem size reached at each time point, based on the zero-growth model36 (see also Figure S2). Colored lines indicate individual trees, faceted by species. Colors correspond with the initial DBH (cm), increasing from smallest (darkest colors) to largest (lightest colors) as indicated in the legend. Start and end dates of each line represent the monitoring period that was retained for each individual after cleaning. **Figure S4:** Relationship between daily max VPD (kPa), soil moisture (VWC, %) and total daily sapflow for 33 individuals. The y-axis displays each tree's total daily sapflow, normalized between 0 and 1, while the x-axis shows the daily maximum vapor pressure deficit (VPD). Color indicates the minimum soil moisture recorded on each day. Each panel represents an individual tree, grouped by species (first top label) and initial DBH (second top label, cm) at the start of the growth measurement period (August 2022). See Section 2 for details. **Figure S5:** Correlation between daily maximum PPFD and VPD. The x axis shows the maximum photosynthetically active radiation (PPFD, mmol/m^2/h) and the y axis the daily maximum VPD (kPa) across the study period. The R^2 value is indicated in the plot. **Figure S6:** Average annual growth by tree DBH. The y-axes shows average annual growth per individual tree (cm), the x-axes represent DBH (cm), faceted by species. The red dots represent the trees from this study, for which we calculated the average hourly growth in their study period and multiplied this by 8760 (24 h × 365 days). The black dots represent trees from the adjacent LFDP 16-ha research plot, where trees are measured every 5 years. Growth for those trees was calculated as the

difference between two censuses, divided by 5 to calculate annual growth and this was averaged for the censuses from 2000 to 2015. **Figure S7:** Posterior predictive model checks of the main model (Figure 2). Posterior predictive checks were performed using the posterior predictive distributions of the model to evaluate how well it captures the observed data. The top panel shows a histogram representing the distribution of the number of days with observed growth across 1000 simulated datasets, with the vertical red line indicating the observed number of growth days. The middle panel presents kernel density estimates of the number of growth hours from 200 simulated datasets, while the red line represents the observed number of growth hours. Similarly, the bottom panel shows kernel density estimates of total daily growth from 200 simulated datasets, with the red line marking the observed daily growth. The close alignment between the simulated distributions and the observed values, highlighted by the red lines, indicates that the model successfully captures the underlying properties of the data. The middle and bottom panels display only 200 simulations, as the original 1000 lines clustered together and obscured details. **Figure S8:** Environmental drivers of radial stem growth response across four tree species, including previous day maximum VPD instead of radiation. Posterior mean coefficients and 95% credible intervals for the effects of four environmental variables on three growth responses: (a) the probability of daily tree growth occurrence, (b) the growth duration (hours) conditional on growth occurrence and (c) the total daily growth (cm) conditional on growth occurrence. Predictor variables include: current day ('growth day 0') maximum soil volumetric water content (VWC, %) and maximum vapor pressure deficit (VPD, kPa), combined with previous day ('growth day −1') maximum VPD (kPa) and photoperiod (hours of daylight). Coefficients were estimated using 1000 draws from the posterior predictive distribution of a Bayesian joint model (Supporting Information S1). **Figure S9:** Environmental drivers of radial stem growth response across four tree species, including both previous day maximum VPD and PPFD depending on the modeled process. Posterior mean coefficients and 95% credible intervals for the effects of four environmental variables on three growth responses: (a) the probability of daily tree growth occurrence, (b) the growth duration (hours) conditional on growth occurrence and (c) the total daily growth (cm) conditional on growth occurrence. Predictor variables include: current day ('growth day 0') maximum soil volumetric water content (VWC, %) and maximum vapor pressure deficit (VPD, kPa), combined with previous day ('growth day −1') maximum VPD (kPa) or maximum photosynthetically active radiation (PPFD, mmol/m^2/h) and photoperiod (hours of daylight). Coefficients were estimated using 1000 draws from the posterior predictive distribution of a Bayesian joint model (Supporting Information S1). **Figure S10:** Environmental drivers of radial stem growth response across four tree species, using daily climate means instead of maxima. Posterior mean coefficients and 95% credible intervals for the effects of four environmental variables on three growth responses: (a) the probability of daily tree growth occurrence, (b) the growth duration (hours) conditional on growth occurrence and (c) the total daily growth (cm) conditional on growth occurrence. Predictor variables include: current day ('growth day 0') mean soil volumetric water content (VWC, %) and mean vapor pressure deficit (VPD, kPa), combined with previous day ('growth day −1') mean photosynthetically active radiation (PPFD, mmol/m^2/h) and photoperiod (hours of daylight). Coefficients were estimated using 1000 draws from the posterior predictive distribution of a Bayesian joint model (Supporting Information S1). **Figure S11:** Species level associations between environmental variables and the probability of growth occurrence with raw data included as dots. Panels show modeled relationships between the probability of observing growth (y-axes) and environmental predictors (x-axes): (a) maximum soil volumetric water content (VWC, %), (b) maximum vapor pressure deficit (VPD, kPa), (c) previous day maximum photosynthetically active radiation (PPFD, mmol/m^2/h) and (d) previous day photoperiod (hours of daylight). Dots show the daily measurements of individual trees. **Figure S12:** Species level associations between environmental variables and growth duration with raw data included as dots. Panels show modeled relationships between the growth duration (hours, y axes) and environmental predictors (x-axes): (a) maximum soil volumetric water content (VWC, %), (b) maximum vapor pressure deficit (VPD, kPa), (c) previous day maximum photosynthetically active radiation (PPFD, mmol/m^2/h) and (d) previous day photoperiod (hours of daylight). Dots show the daily measurements of individual trees. **Figure S13:** Species level associations between environmental variables and total daily radial stem growth with raw data included as dots. Panels show modeled relationships between predicted daily growth (cm, y-axes) and environmental predictors (x-axes): (a) maximum soil volumetric water content (VWC, %), (b) maximum vapor pressure deficit (VPD, kPa), (c) previous day maximum photosynthetically active radiation (PPFD, mmol/m^2/h) and (d) previous day photoperiod (hours of daylight). Dots show the daily measurements of individual trees.